ISSN 0031-918X, Physics of Metals and Metallography, 2017, Vol. 118, No. 7, pp. 621–629. © Pleiades Publishing, Ltd., 2017.
Original Russian Text © R.T. Murzaev, D.V. Bachurin, A.A. Nazarov, 2017, published in Fizika Metallov i Metallovedenie, 2017, Vol. 118, No. 7, pp. 655–664.

THEORY OF METALS

Relaxation of the Residual Defect Structure in Deformed Polycrystals under Ultrasonic Action

R. T. Murzaev[a, *], D. V. Bachurin[a, b], and A. A. Nazarov[a, c]

[a] *Institute for Metals Superplasticity Problems, Russian Academy of Sciences, ul. Khalturina 39, Ufa, 450001 Bashkortostan, Russia*

[b] *Institute for Applied Materials, Karlsruhe Institute of Technology, Hermann-von-Helmholtz-Platz 1, Eggenstein-Leopoldshafen, 76344 Germany*

[c] *Bashkir State University, ul. Zaki Validi 32, Ufa, 450074 Bashkortostan, Russia*

**e-mail: mur611@mail.ru*

Received June 28, 2016; in final form, December 28, 2016

Abstract—Using numerical computer simulation, the behavior of disordered dislocation systems under the action of monochromatic standing sound wave has been investigated in the grain of the model two-dimensional polycrystal containing nonequilibrium grain boundaries. It has been found that the presence of grain boundaries markedly affects the behavior of dislocations. The relaxation process and changes in the level of internal stresses caused by the rearrangement of the dislocation structure due to the ultrasonic action have been studied.

Keywords: disordered dislocation systems, dislocation slip, disclination quadrupole, ultrasound, ultrasonic treatment

DOI: 10.1134/S0031918X17070079

INTRODUCTION

Numerous experimental investigations show that ultrasonic treatment brings about substantial changes in the dislocation structure of crystalline materials [1–4]. At high ultrasonic amplitudes these changes are associated with the intense generation of dislocations and the formation of the cellular structure [2, 5–7], the nucleation of fatigue cracks and fracture [8], and the strengthening of materials [4]. Upon intense ultrasonic treatment, the nanostructuring of the surface can occur [9, 10]. For moderate amplitudes not exceeding the dynamic yield strength, the relaxation of internal stresses related to the redistribution of dislocations and the formation of a more equilibrium structure takes place, which in turn leads to a reduction in the strength and plasticization of materials [11].

The formation of nanostructured near-surface layers and growth in their microhardness by 10–80% was found in copper after ultrasonic treatment in [10]. Ultrasonic vibrations used in situ upon the tensile deformation of low-carbon steels cause a considerable decrease in both the dislocation density and fraction of low-angle grain boundaries [12]. In the authors' opinion, these microstructural changes are due to the increased mobility of dislocations and, hence, to a higher probability of the annihilation of dislocation dipoles. An increase in the hardness by 14%, the elasticity modulus by 9%, and thermal stability due to structural relaxation likewise takes place in metallic glasses upon ultrasonic treatment [13].

The relaxing influence of ultrasound on the structure of nanocrystalline and ultrafine-grained materials produced by severe plastic deformation was investigated in [14–16]. Using X-ray diffraction analysis, the authors measured the root-mean-square elastic deformation in the samples and detected its significant decrease after treatment by ultrasound of different amplitude. Tests for impact toughness of nickel preliminarily subjected to equal-channel angular pressing with subsequent ultrasonic treatment showed an increase in the fracture energy more than sevenfold as compared to the nonsonicated sample [14]. In a Zr–2.5% Nb alloy with the nanodimensional structure of deformation origin, it was revealed that, after ultrasonic treatment, the level of internal stresses decreased markedly with the retention of ultrafine-grained morphology and an enhancement in the general structural homogeneity [17].

A more comprehensive study of mechanisms of the formation and dynamics of elementary dislocation structures, such as dislocation dipoles and multipoles, was performed theoretically, including the computer simulation method. The action of the monochromatic standing sound wave on the dislocation dipoles (two edge dislocations of opposite sign) was investigated in [18–20]. Note that no translational motion of disloca-

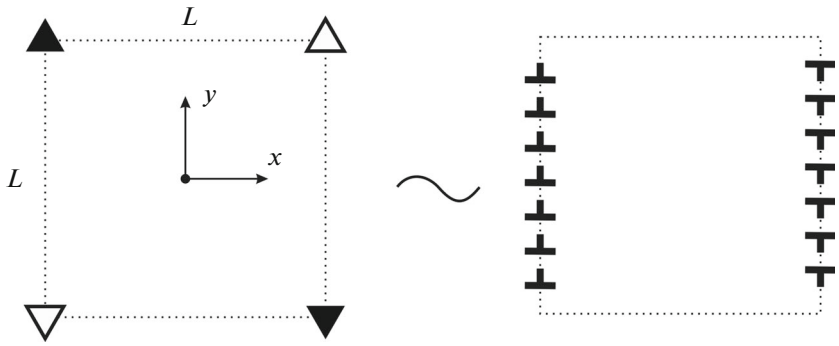

Fig. 1. Two walls of edge dislocations with Burgers vectors that are equal in magnitude and opposite in sign and a disclination quadrupole equivalent to them. Black triangles designate positive junction disclinations; white triangles designate negative disclinations. The coordinate system used in this work is also shown. Dashed lines image a square grain in the model two-dimensional polycrystal.

tion dipoles was detected. Recently, the authors of [21, 22] investigated the dynamics of the motion of different tripole configurations (one dislocation has a sign opposite to the sign of the other two), which, as was shown, can drift under the action of the standing sound wave and mutually transform into each other.

Large disordered dislocation ensembles under the ultrasonic action with their subsequent rearrangement into dynamically ordered walls were simulated in [7, 23–27]. It was revealed that the formation of these dislocation walls occurs upon the slip of both single dislocations and dislocations constituting multipole configurations and after cessation of the ultrasonic action the formed structures did not decompose. The similar ordered dislocation ensembles formed due to the ultrasonic action were also observed experimentally [7].

In the above-cited works the behavior of dislocation systems was in essence simulated in an infinite single crystal without taking into account grain boundaries including those with the nonequilibrium structure, i.e., creating long-range stress fields. Studying rearrangements of dislocation systems in polycrystals with grain boundaries exhibiting the defect structure is of considerable interest for understanding mechanisms of the ultrasonic action on the structure of bulk nanomaterials. In this work using numerical simulation the evolution of disordered dislocation systems in the separate grain of polycrystal was investigated under the ultrasonic action with allowance for nonequilibrium state of grain boundaries. The problem is solved within the discrete-dislocation approach.

DESCRIPTION OF THE MODEL

The velocity of motion of the straight edge dislocation is described by the empirical expression [28]

$$V = B|\tau|^m \operatorname{sgn}(\tau), \quad (1)$$

where B is the dislocation mobility factor, m is the characteristic that at low shear stresses is equal to a few units, and τ is the total shear stress in the slip plane of the dislocation in the direction of the Burgers vector. Shear stresses of a single edge dislocation with the Burgers vector $\mathbf{b} = (b, 0, 0)$ in planes parallel to the slip plane have the form [29]

$$\tau(x, y) = Db\frac{x(x^2 - y^2)}{(x^2 + y^2)^2}, \quad (2)$$

where $D = \mu/2\pi(1 - \nu)$ and μ and ν are the shear modulus and Poisson ratio, respectively.

Let some system of n edge dislocations be subjected to the external alternating stress field $\tau(t)$ that satisfies the following conditions:

(1) $\tau(t)$ is homogeneous within the region of dislocation motion, i.e., the standing sound wave with a length that greatly exceeds possible amplitudes of dislocation motion affects the dislocation system.

(2) The amplitude of alternating stresses is below the threshold value (dynamic yield strength) so that no dislocations are generated and their density does not increase.

(3) The velocity of the dislocation motion is small compared to the sound velocity in the medium so that relativistic effects can be neglected.

In addition, we neglect the influence of the crystallographic orientation of samples on the dynamics of dislocations and the influence of impurity atoms and other defects of all kinds and consider only dislocation slip completely ignoring climbing.

Let us consider a model two-dimensional polycrystal that consists of square grains and one grain of this polycrystal. Assume that the boundaries of this grain contain a mesodefect, the stress field of which is described using a quadrupole of wedge junction disclinations (Fig. 1). This mesodefect can be formed upon the plastic deformation of polycrystals [30] and is a characteristic element of the nonequilibrium structure

of ultrafine-grained materials produced by severe plastic deformation [31].

Let us choose the coordinate system in the same manner as is shown in Fig. 1. Let the X axis be the direction of dislocation motion. Let us denote the coordinate of the i-th dislocation by x_i and the shear stress produced by the i-th dislocation at the location of the j-th dislocation by τ_{ij}. The τ_{ij} value is determined by formula (2). For simplicity, we take m to be an odd integer number. Then, the system of equations of motion for the i-th dislocation of the system is written as

$$\frac{dx_i}{dt} = B\left(S_i\tau(t) + \sum_{\substack{j=1\\ j\neq i}}^{n}\tau_{ji}(x_i - x_j, y_i - y_j) + \tau_{xy}^{\text{quad}}(x,y)\right)^m. \quad (3)$$

Here, $S_i = \pm 1$ depending on the sign of a dislocation; n is the total number of dislocations; $\tau(t)$ is an external stress (induced by the ultrasonic action in this case) that varies according to the sinusoidal law $\tau(t) = \tau_0 \sin\omega t$, where τ_0 and ω are the amplitude and frequency, respectively. The phase shift is set equal to zero, which corresponds to a standing wave. Here, it is also taken into account that $\tau_{ji} = \tau_{ij}$. Note that expression (3) contains no term related to the maximum dry friction force, i.e., the start stress at which dislocations begin their motion. Allowing for the dry friction force affects the velocity of system dislocations, does not influence the general picture of relaxation, and is a separate problem that was considered previously in [32]. The shear stress field of the disclination quadrupole $\tau_{xy}^{\text{quad}}(x,y)$, which is composed of disclinations with the strength Ω and arm L, is determined by the expression [33]

$$\tau_{xy}^{\text{quad}}(x,y) = -D\Omega\left(\frac{(x-L)(y-L)}{(x-L)^2 + (y-L)^2} - \frac{(x+L)(y-L)}{(x+L)^2 + (y-L)^2} + \frac{(x+L)(y+L)}{(x+L)^2 + (y+L)^2} - \frac{(x-L)(y+L)}{(x-L)^2 + (y+L)^2}\right). \quad (4)$$

In order to numerically solve the system of equations (3), it is convenient to use dimensionless variables: $\tilde{t} = \omega t$ for time and $\tilde{x} = x\omega/B\tau_0^m$ for coordinates. Let us also represent stresses $\tau_{ij}(x_j - x_i, y_j - y_i)$ and $\tau_{xy}^{\text{quad}}(x,y)$ in terms of the universal functions $f(x,y)$ and $g(x,y)$ depending only on the coordinates

$$\tau_{ij}(x_j - x_i, y_j - y_i) = Dbf_{ij}(x_j - x_i, y_j - y_i), \quad (5)$$

where

$$f(x,y) = \frac{x(x^2 - y^2)}{(x^2 + y^2)^2}$$

and

$$\tau_{xy}^{\text{quad}}(x,y) = -D\Omega g(x,y), \quad (6)$$

where

$$g(x,y) = \frac{(x-L)(y-L)}{(x-L)^2 + (y-L)^2} - \frac{(x+L)(y-L)}{(x+L)^2 + (y-L)^2} + \frac{(x+L)(y+L)}{(x+L)^2 + (y+L)^2} - \frac{(x-L)(y+L)}{(x-L)^2 + (y+L)^2}.$$

After the substitution of expressions (5) and (6) and elementary transformations, the system (3) takes on the form

$$\frac{d\tilde{x}_i}{d\tilde{t}} = \left(S_i \sin\tilde{t} + \frac{Db\omega}{B\tau_0^{m+1}} \times \sum_{\substack{j=1\\ j\neq i}}^{n} f_{ji}(\tilde{x}_i - \tilde{x}_j, \tilde{y}_i - \tilde{y}_j) + \frac{D\Omega}{\tau_0} g(\tilde{x},\tilde{y})\right)^m. \quad (7)$$

Each equation in the system (7) written in dimensionless coordinates depends on two parameters. The first of them, $K = Db\omega/B\tau_0^{m+1}$, which is responsible for the interdislocation interaction, contains two independent parameters, i.e., frequency ω and amplitude τ_0 of external stresses; numerous values of the pair ω and τ_0 can correspond to one value of the parameter K. The second parameter $Q = D\Omega/\tau_0$, which is related to the presence of the disclination quadrupole, depends on the pair Ω and τ_0.

The system of equations (7) was solved numerically by the Runge–Kutta fourth-order method. In doing so, the following parameters of the model and initial conditions were used. As was shown earlier [21, 22], the nonlinearity of the dependence (1) is a necessary condition for drift of dislocation tripoles. With allowance for this and also for the convenience of considering changes in the direction of velocity when the stress sign changes, the exponent of the stress was chosen to be equal to $m = 3$. This relationship describes the dependence of the velocity of dislocations on the stress in α iron at room temperature fairly well [28]. The integration step was chosen equal to $dt = 2\pi \times 0.0001/\omega$. To estimate the coefficients K and Q, we used the following values of main parameters for α iron: $B = 10^{-5}$ Pa s, $b = 2.482$ Å, $\mu = 82$ GPa, $\nu = 0.29$, $\Omega = 1°–2°$, and $\tau_0 < \mu/2$. It was assumed that, at the initial time instant, all dislocations exhibit zero values of the velocity.

The initial distribution of dislocations in disordered ensemble and their signs were specified randomly. Since all dislocations in the initial configuration belong to one slip system, although they are located in different (parallel) slip planes, the annihilation of two dislocations with opposite Burgers vectors is excluded within this model. Assuming that the typical interdislocation distance is on the order of $10b$ and the quadrupole arm is about 600 interdislocation distances, the size of the simulated grain is 150 nm. Then, 50 dislocations in the computational cell correspond to the dislocation density around 2.2×10^{13} m^{-2}; 500 dislocations, to the dislocation density around 2.2×10^{14} m^{-2}.

In order to estimate the degree of relaxation of the dislocation system, the root-mean-square value of the sum of diagonal components (spur) of the internal stress tensor was calculated in the grain via averaging over mesh nodes composed of $N = 100 \times 100$ points as follows:

$$\left\langle Sp\sigma^2_{\text{total}} \right\rangle^{1/2} = \frac{1}{N}\sqrt{\sum_{i=1}^{N}\left(\sum_{j=xx,yy,zz} \sigma_j^{disl}(x,y) + \sum_{j=xx,yy,zz} \sigma_j^{\text{quad}}(x,y) \right)^2} = \frac{D(1+\nu)}{N}\sqrt{\sum_{i=1}^{N}\left(H(x,y,x_i,y_i,L)\right)^2}, \quad (8)$$

where

$$H(x,y,x_i,y_i,L) = -2b\sum_{i=1}^{n}\frac{y-y_i}{(x-x_i)^2+(y-y_i)^2} + \Omega \ln\frac{((x-L)^2+(y-L)^2)((x+L)^2+(y+L)^2)}{((x+L)^2+(y-L)^2)((x-L)^2+(y+L)^2)}. \quad (9)$$

In our calculations, we discarded the mesh nodes that are located at distances shorter than $0.1b$ from the core of the dislocation or disclination.

When the behavior of the dislocation system in the grain surrounded by high-angle boundaries was simulated, it was assumed that the dislocation falling in planes $x = -L$ and $x = L$ remains there over the course of the whole further simulation time. This reflects the fact that grain boundaries are sinks for dislocations. Transparent boundaries that do not present obstacles to dislocation motion were also simulated for comparison.

SIMULATION RESULTS

Figure 2a displays the initial configuration composed of randomly distributed dislocations. Calculations with impenetrable boundaries performed for a large number of systems with different parameters showed that, under ultrasonic action, the considerable rearrangement of the dislocation structure takes place, namely, all dislocations begin to move from the grain interior into grain boundaries (see Fig. 2b). Upon motion dislocations can unite into tripoles and more complex multipole configurations. Previously, in [21, 22], we studied the former configurations in detail. In this case, positive dislocations move toward the right-hand boundary, while negative dislocations move toward the left-hand boundary. This behavior is directly connected with the stress field of the disclination quadrupole. After ultrasonic action, all dislocations (or the majority of them) are found to be at the grain boundaries, as is shown in Fig. 2c. Note that, at low strengths of disclinations in the quadrupole and at low amplitudes of the external ultrasonic action, only dislocations located in the immediate vicinity of grain boundaries can be absorbed, whereas the other dislocations located closer to the center of the grain that unite into dipoles and more complex configurations remain practically immobile (see Fig. 2b). Some of the observed configurations are merely dislocation walls that consist of dislocations of the same sign. The formed dislocation structures are stable and do not decompose after the cessation of ultrasonic action. At high amplitudes of the external action, these multipole configurations do not arise inside of grains. All dislocations enter into the grain boundaries; i.e., a more careful cleaning of grains by ultrasound occurs.

If the slip plane of a lattice dislocation is close to the slip plane of a dislocation located in the wall to this time instant, this lattice dislocation due to elastic repulsive forces cannot be incorporated into the dislocation wall; rather, it stops at some distance from it. The appearance of other lattice dislocations with close-spaced slip planes gives rise to dislocation pileups near the grain boundary. The example of this pileup of two dislocations is shown in Fig. 2 in the lower right-hand corner adjacent to the positive disclination.

Figure 2d shows the result of simulating the behavior of dislocations in the grain with penetrable boundaries. It can be seen that dislocations form walls that bend under ultrasonic action. In real crystals this means the possibility of grain-boundary migration. At high amplitudes of the ultrasonic action, such walls can be destroyed easily and individual dislocations of these walls can be absorbed by neighboring boundaries, which ultimately results in the softening of the material. Note that, if we remove the ultrasonic

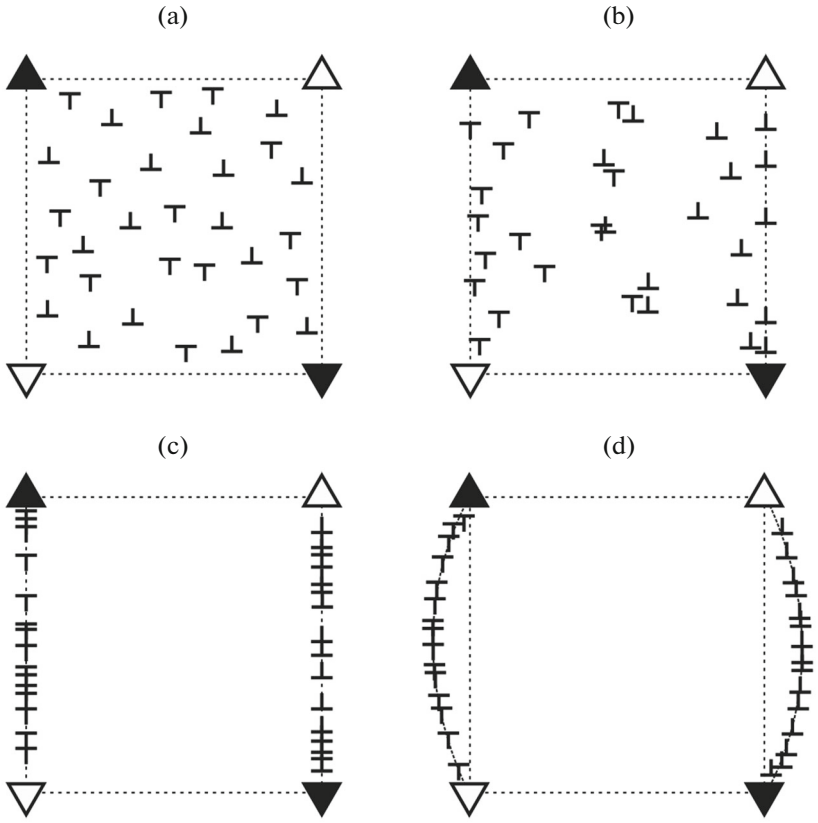

Fig. 2. Arrangement of dislocations in the computational cell: (a) initial disordered distribution of dislocations (n = 31) and (b) in the process of their motion to grain boundaries under the ultrasonic action. At the center of the grain, dislocation dipoles and tripoles that arise when slip planes of dislocations are in close proximity are seen; (c) after the ultrasonic action when dislocations cannot pass through grain boundaries (the case of high-angle grain boundaries); (d) when grain boundaries are penetrable (the case of low-angle grain boundaries). Black triangles designate positive junction disclinations; white triangles show negative disclinations. Dashed lines image the square grain in the model two-dimensional polycrystal.

action, configuration in Fig. 2d rather rapidly takes on the form depicted in Fig. 2c.

A time dependence of the root-mean-square spur of the stress tensor in each oscillation period for configurations with different number of dislocations is shown in Fig. 3. It can be seen that this quantity changes nonmonotonously and at some time instants the subsequent value can exceed the previous value. This stems from the fact that the spur is calculated only once within the whole oscillation period and at this time instant dislocations are not necessarily located in stable positions. An analysis of different dislocation configurations with different set of parameters shows that the root-mean-square spur of the system with minor number of dislocations (n = 50) decreases substantially more strongly than in systems with a greater dislocation density (n = 200 and 500). In the latter case this is connected with the formation of a dislocation substructure that consists of immobile dipoles and multipoles. For the case shown in Fig. 3, the relaxation of root-mean-square stresses is about 24% for n = 50, about 11% for n = 200, and about 4% for

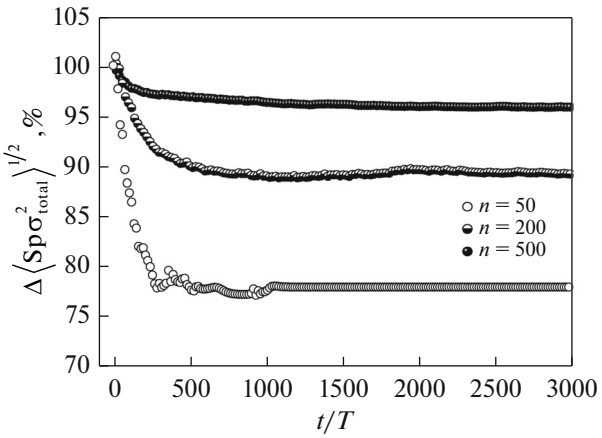

Fig. 3. Dependence of the relative change in the root-mean-square spur of the stress tensor of dislocations on time (in oscillation periods T) calculated for a system of n = 50, 200, and 500 dislocations under the ultrasonic action. Spur value in the initial configuration was taken to be 100%. Other parameters of the system are $1/K = 0.2$ and $Q = 0.3$.

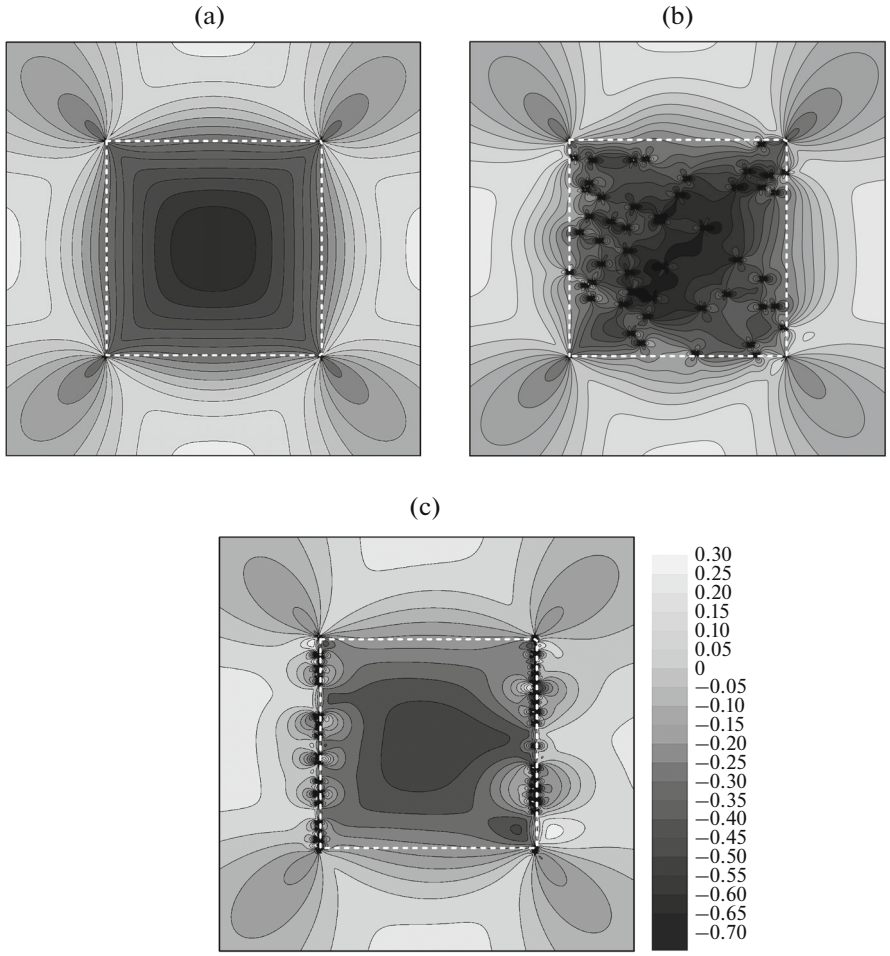

Fig. 4. Maps of the shear stress-field component σ_{xy}: (a) pure disclination quadrupole not containing a disordered ensemble of lattice dislocations, (b) disordered system of 50 dislocations before the ultrasonic action, and (c) the same system after ultrasonic action. Dashed line delineates the square grain, where disclinations are located at the corners. Stresses are expressed in dimensionless units.

$n = 500$. Note that these values should be considered as approximate, since they were obtained for an ideal system of straight dislocations that do not contain point and linear defects that could exert a retarding influence on the glide lattice dislocations. In addition, the relaxation rate of dislocation systems would likewise depend on the amplitude and frequency of an external load.

Maps of the shear component of the stress field, σ_{xy}, in the grain with the presence of the pure disclination quadrupole (without a system of lattice dislocations) and in the grain that contains a quadrupole and a disordered system of dislocations are depicted in Fig. 4 before and after ultrasonic action. It can be seen that, in the initial configuration in Fig. 4b, the level of stresses inside the grain is rather inhomogeneous and is generally higher than in the pure disclination quadrupole (see Fig. 4a). A more homogeneous stress field inside the grain compared to Fig. 4b is characteristic of the final configuration obtained after ultrasonic treatment (Fig. 4c). It is clearly seen that lattice dislocations that reached grain boundaries and formed flat dislocation walls partially reduce the long-range stress field of disclinations and significantly decrease the stresses in the grain interior (see Fig. 4c).

In order to reveal how much the influence of ultrasound can change internal elastic stresses in grain, the initial and final values of the root-mean-square spur for different randomly distributed systems of dislocations were calculated; then, average values were obtained from them. Here, the parameters K and Q were specially selected so that all dislocations could enter into grain boundaries. Two dislocation densities (2.2×10^{13} m^{-2} and 2.2×10^{14} m^{-2}) were considered and 50 calculations were performed for each of them. It can be seen in Fig. 5 that, on average, the root-mean-square spur of the stress tensor changes by approximately 12–20% of the initial value. As the initial dislocation density increases, the scatter of the spur values decreases approximately from ±8 to ±5%.

RESULTS AND DISCUSSION

The behavior of disordered dislocation systems in finite-size grains under ultrasonic action, which was considered in this work, significantly differs from the findings detected previously in infinite crystals [7, 23–26]. In the latter, the walls that alternated in the Burgers vector sign of dislocations composing these walls were formed of like dislocations (see Fig. 5 in [7]). This is primarily connected with the presence of stress fields of nonequilibrium grain boundaries that attract lattice dislocations and are sinks for them. Thus, it can be concluded that the arrangement of dislocations described by the authors of [7] can only be observed in rather large grains and away from boundaries, whereas in small grains and in the immediate vicinity of boundaries, dislocations are absorbed by the grain boundaries.

The process of the relaxation of the dislocation structure (see Fig. 3) can be conditionally separated into two stages. The first stage is when the root-mean-square spur of the stress tensor falls off rapidly by an approximate linear law that corresponds to motion of the majority of dislocations toward grain boundaries. The second stage is when the majority of dislocations were already absorbed by boundaries and remaining single dislocations or more complex multipole configurations continue to drift slowly toward boundaries. Two causes are primarily responsible for this slow motion. The first is the almost complete lack of influence of an external alternating field on single dislocations that do not form multipoles, since their displacement in one direction is completely compensated by displacement in opposite direction. The immobility of dislocation dipoles and walls can be explained based on a criterion formulated earlier in [21, 22], namely, the lack of asymmetry in the arrangement of centers of masses of positive and negative dislocations. The second is that, since the disclination quadrupole and formed dislocation walls in boundaries that compensate for the stress field of disclinations create no long-range stress fields, the total average stress that affects single dislocations and multipoles is relatively small.

When investigating the self-organization of dislocations in ultrasonic fields, the authors of [7] found that there is some characteristic time after which the total percentage of dislocations incorporated into walls remains unaltered. Namely, after about 70 oscillation periods, ~70–80% of the total number of dislocations in an ensemble embed into walls. This agrees fairly well in time and number of dislocations with the above-described first (rapid) stage of the relaxation of the disordered dislocation system located in the disclination quadrupole field.

In [15, 16, 34], the ultrasonic action on the structure and mechanical properties of nanostructured nickel obtained by high pressure torsion and ultrafine-grained nickel produced by equal-channel angular pressing were studied experimentally. In the first case,

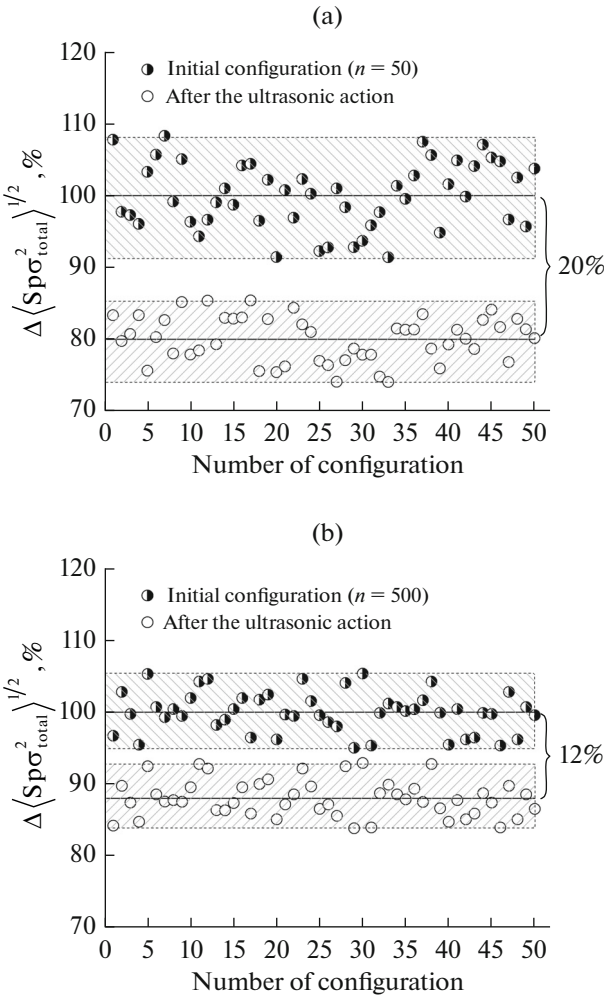

Fig. 5. Relative change in the root-mean-square spur of the stress tensor of dislocations calculated in the initial state and after ultrasonic action for 50 different dislocation configurations with different number of dislocations: (a) n = 50 and (b) n = 500. Average spur value in the initial configuration was taken to be 100%. Horizontal lines show average spur values before and after the ultrasonic action. Shaded regions illustrate a scatter of spur values. Number on the right indicates how much (in percentage) the stress tensor spur changed. Other parameters of the system are $1/K = 0.7$ and $Q = 0.3$.

a decrease in the root-mean-square elastic deformation by 10–47% and in the second case by 10–16% was revealed in a wide range of ultrasound amplitudes. This decrease in internal stresses can be explained based on the relaxation of the total defect structure of deformed polycrystal that consists of the system of junction disclinations and lattice dislocations. Thus, the estimate (we obtained above) of changes in the stress tensor spur in the range of 4–20% (see Figs. 3, 5) fairly well falls within the range of experimental values. Such high relaxation of the root-mean-square deformation (up to 47%) in [16] can be caused by either a high density of lattice dislocations or the ultrasonic action on

other relaxation processes. The number of oscillation periods required to achieve such relaxation differs by three orders of magnitude, i.e., about 100–300 in this work (which corresponds to the end of the first stage, see Fig. 3) and 6.6×10^5 (ultrasound frequency 22 kHz and operation time 30 s) in [15, 16, 34]. Unfortunately, no experimental data on the dependence of the degree of relaxation on the time of ultrasonic action are available. However, the data of this work show that, in experiments, the main operation effect can occur for much shorter time lapse than 30 s.

The considered mechanism of relaxation of the nonequilibrium structure of deformed polycrystals differs greatly from the mechanism of recovery of the structure of nonequilibrium grain boundaries upon annealing. As is shown in [35, 36], upon annealing, the system of junction disclinations relaxes via the redistribution of dislocations in a network of grain boundaries and is controlled by grain-boundary diffusion. This process occurs at high temperature and very long-duration, whereas relaxation upon ultrasonic treatment can occur athermally and appreciably faster.

In this work, a simplified model of the grain with one principal slip plane that exhibits the maximum Schmidt factor was used. However, in real crystals, there are always other equivalent slip planes (not parallel to the above plane) with smaller orientation factors. It is obvious that dislocations located at these planes interact with dislocations of the principal plane, which can lead to changes in the kinetics of the relaxation process. In particular, dislocation pileups presenting obstacles for dislocation motion can be formed. Studying the relaxation of these systems with different equivalent slip planes is doubtless a topical problem of physical materials science that calls for separate consideration.

In conclusion, it should be noted that, under the action of standing sound waves, internal stresses connected with the redistribution of lattice dislocations in the field of nonequilibrium grain boundaries experience relaxation. The majority of dislocations enters into boundaries and constitutes a wall that compensates for long-range stress fields of junction disclinations. The other dislocations can form stable immobile configurations that at high amplitudes of the ultrasonic action can reach grain boundaries. The understanding of relaxation mechanisms of the residual defect structure in deformed polycrystals makes it possible to choose the optimum regime of ultrasonic treatment of materials and, thus, markedly affect their mechanical properties.

CONCLUSIONS

(1) Allowance for stress fields of grain boundaries results in the qualitatively different behavior of disordered dislocation systems under ultrasonic action compared to the behavior of systems in an infinite-size single crystal.

(2) Entering in nonequilibrium boundaries dislocations under the ultrasonic action constitute a perfect flat dislocation wall that does not create long-range stress fields.

(3) The relaxation of the disordered dislocation structure can be conditionally separated into two stages, i.e., the rapid stage when the majority of dislocations move in the direction of grain boundaries and are absorbed by them and the slow stage related to the drift of remaining single dislocations and their clusters.

(4) Due to the ultrasonic action, a considerable decrease in the level of internal stresses connected with the relaxation of the dislocation structure takes place.

ACKNOWLEDGMENTS

R.T. Murzaev and A.A. Nazarov are greatful to grant no. 16-19-10126 for financial support.

REFERENCES

1. K. H. Westmacott and B. Langenecker, "Dislocation structure in ultrasonically irradiated aluminum," Phys. Rev. Lett. **14**, 221–225 (1965).
2. N. A. Tyapunina, E. K. Naimi, and G. M. Zinenkova, *Action of Ultrasound on Crystals with Defects* (Izd. MGU, Moscow, 1999) [in Russian].
3. V. P. Severdenko, V. V. Klubovich, and A. V. Stepanenko, *Treatment of Metals by Pressure with Ultrasound* (Nauka i Tekhnika, Minsk, 1973) [in Russian].
4. A. V. Kulemin, *Ultrasound and Diffusion in Metals* (Metallurgiya, Moscow, 1978) [in Russian].
5. O. V. Abramov, *Influence of Strong Ultrasound on Liquid and Solid Metals* (Nauka, Moscow, 2000) [in Russian].
6. S. V. Kovsh, V. A. Kotko, I. G. Polotskii, G. I. Prokopenko, V. I. Trefilov, and S. A. Firstov, "Influence of ultrasound on the dislocation structure and mechanical properties of molybdenum," Fiz. Met. Metalloved. **35**, 1199–1205 (1973).
7. G. V. Bushueva, G. M. Zinenkova, N. A. Tyapunina, V. T. Degtyarev, A. Yu. Losev, and F. A. Plotnikova, "Self-organization of dislocations in an ultrasound field," Crystal. Rep. **53**, 474–479 (2008).
8. I. G. Polotskii, V. F. Belostotskii, and O. N. Kashevskaya, "Action of ultrasound radiation on the hardness of nickel single crystals," Fiz. Khim. Obrab. Mater. no. 4, 152–155 (1971).
9. A. I. Lotkov, A. A. Baturin, V. N. Grishkov, Zh. G. Kovalevskaya, and P. V. Kuznetsov, "Effect of ultrasonic plastic treatment on the surface structure and phase state of titanium nickelide," Tech. Phys. Lett. **31**, 912–914 (2005).
10. V. K. Astashev and V. L. Krupenin, "On the optimization of vibro-impact processes in lattice structures," Vestn. Nizhegorod.Univ., nos. 4–5, 1975–1977 (2011).
11. A. V. Mats, V. M. Netesov, V. I. Sokolenko, and K. V. Kovtun, "Relaxation effects in strained hafnium

under ultrasonic treatment," Vopr. At. Nauki Tekh., Ser.: Fiz. Radiat. Povrezhd.. Radiat. Materialoved.., no. 4, 167–169 (2009).

12. R. K. Dutta, R. H. Petrov, R. Delhez, M. J. M. Hermans, I. M. Richardson, and A. J. Böttger, "The effect of tensile deformation by in situ ultrasonic treatment on the microstructure of low-carbon steel," Acta Mater. **61**, 1592–1602 (2013).
13. Y. Wang, W. Zhao, G. Li, and R. Liu, "Effects of ultrasonic treatment on the structure and properties of Zr-based bulk metallic glasses," J. Alloys Compd. **544**, 46–49 (2012).
14. A. A. Samigullina, R. R. Mulyukov, A. A. Nazarov, A. A. Mukhametgalina, Yu. V. Tsarenko, and V. V. Rubanik, The increase of impact strength of ultrafine grained nickel after ultrasonic treatment," Lett. Mater. **4**, 52–54 (2014).
15. A. A. Nazarova, R. R. Mulyukov, V. V. Rubanik, Yu. V. Tsarenko, and A. A. Nazarov, "Effect of ultrasonic treatment on the structure and properties of ultrafime-grained nickel," Phys. Met. Metallogr. **110**, 574–581 (2010).
16. A. A. Nazarov, A. A. Samigullina, R. R. Mulyukov, Yu. V. Tsarenko, V. V. Rubanik, "Changes in the microstructure and mechanical properties of nanomaterials under an ultrasonic wave effect," J. Machinery Manufact. Reliability **43**, 153–159 (2014).
17. A. V. Mats, V. M. Netesov, and V. I. Sokolenko, "Ultrasonic influence on nanostructure of Zr–2.5% Nb alloy," Vopr. At. Nauki Tekh., Ser.: Fiz. Radiats. Povrezhd. Radiats. Materialoved. Sci., no. 4, 108–110 (2011).
18. G. M. Zinenkova, A. L. Lomakin, and Kh. Khristu, *Computer Simulation of Structural Effects in Crystals* (Leningrad. Izd. FTI im. Ioffe, Leningrad, 1988) [in Russian].
19. N. A. Tyapunina, A. L. Lomakin, and Kh. Khristu, "Dynamic structures of dislocation dipoles under ultrasonic treatment," Fiz. Tverd. Tela **32**, 1097–1101 (1990).
20. Kh. Khristu, *Candidate Sci. (Math.-Phys.) Dissertation* (MGU, Moscow, 1991).
21. R. T. Murzaev, D. V. Bachurin, and A. A. Nazarov, "Interaction of dislocation tripoles with a standing sound wave," Phys. Met. Metallogr. **116**, 1057–1065 (2015).
22. R. T. Murzaev, D. V. Bachurin, and A. A. Nazarov, "Drift of dislocation tripoles under ultrasound influence," Ultrasonics **64**, 77–82 (2016).
23. V. T. Degtyarev, "Self-organization of dislocation ensembles in an ultrasonic field," Mater. Electr. Tekh., Izv. VUZov, no. 1, 34–37 (2004).
24. V. T. Degtyarev, A. Yu. Losev, F. A. Plotnikov, and N. A. Tyapunina, "Modelling of polygonization in ultrasound field," Izv. Akad. Nauk, Ser. Fiz. **68**, 1516–1517 (2004).
25. V. T. Degtyarev, A. Yu. Losev, and F. A. Plotnikov, "Dynamic dislocation structures in the ultrasound field," Materialovedenie, no. 7, 8–12 (2004).
26. V. T. Degtyarev, A. Yu. Losev, and F. A. Plotnikov, "Redistribution of non-ordered dislocation ensembles in the ultrasound field," Naukoem. Tekhnol. **6**, 5–7 (2005).
27. F. A. Plotnikov and D. V. Manukhina, "Mathematical simulation of the process of self-organization of forest dislocation in an ultrasound field," Vestn. TGU **18**, 1879–1880 (2013).
28. A. N. Orlov, *Introduction into the Theory of Defects in Crystals* (Vysshaya Shkola, Moscow, 1983) [in Russian].
29. J. P. Hirth and J. Lothe, *Theory of Dislocations* (McGraw-Hill, New York,1968; Atomizdat, Moscow, 1972).
30. V. V. Rybin, *Large Plastic Deformation and Fracture of Metals* (Metallurgiya, Moscow, 1986) [in Russian].
31. A. A. Nazarov, R. Z. Valiev, and A. E. Romanov, "Random disclination ensembles in ultrafine-grained materials produced by severe plastic deformation," Scr. Mater. **34**, 729–734 (1996).
32. A. A. Nazarov and Sh. Kh. Khannanov, "Ultrasound stimulation of the polygonization process," Fiz. Khim. Obr. Mater., no. 4, 109–114 (1986).
33. V. I. Vladimirov and A. E. Romanov, *Disclinations in Crystals* (Nauka, Leningrad, 1986) [in Russian].
34. A. A. Samigullina, A. A. Nazarov, R. R. Mulyukov, Yu. V. Tsarenko, and V. V. Rubanik, "Effect of ultrasonic treatment on the strength and ductility of bulk nanostructured nickel processed by equal-channel angular pressing," Rev. Adv. Mater. Sci. **39**, 48–53 (2014).
35. A. A. Nazarov and D. V. Bachurin, "On the relaxation of quadrupoles of junction disclinations in deformed polycrystals," Phys. Met. Metallogr. **96**, 446–451 (2003).
36. D. V. Bachurin and A. A. Nazarov, "On the annealing of junction disclinations in deformed polycrystals," Philos. Mag. **83**, 2653–2667 (2003).

Translated by I. Krasnov